BIOTECHNOLOGY
BIOENGINEERING WILEY

A proteomics approach to decipher a sticky CHO situation

Swetha Kumar[1] | Amit Kumar[2] | Steven Huhn[2] | Lauren DeVine[3] |
Robert Cole[3] | Zhimei Du[2] | Michael Betenbaugh[1]

[1]Department of Chemical and Biomolecular Engineering, Johns Hopkins University, Baltimore, Maryland, USA

[2]Process Cell Sciences, Merck & Co. Inc., Kenilworth, New Jersey, USA

[3]Mass Spectrometry and Proteomics Facility, Department of Biological Chemistry, Johns Hopkins University School of Medicine, Baltimore, Maryland, USA

Correspondence
Michael Betenbaugh, Department of Chemical and Biomolecular Engineering, Johns Hopkins University, Baltimore, MD, USA.
Email: beten@jhu.edu

Funding information
Merck Sharp & Dohme LLC, a subsidiary of Merck & Co., Inc., Rahway, NJ, USA

Abstract

Chinese hamster ovary (CHO) cells serve as protein therapeutics workhorses, so it is useful to understand what intrinsic properties make certain host cell lines and clones preferable for scale up and production of target proteins. In this study, two CHO host cell lines (H1, H2), and their respective clones were evaluated using comparative TMT-proteomics. The clones obtained from host H1 showed increased productivity (6.8 times higher) in comparison to clones from host H2. Based on fold-change analyses, we observed differential regulation in pathways including cell adhesion, aggregation, and cellular metabolism among others. In particular, the cellular adhesion pathway was downregulated in H1, in which podoplanin, an antiadhesion molecule, was upregulated the most in host H1 and associated clones. Phenotypically, these cells were less likely to aggregate and adhere to surfaces. In addition, enzymes involved in cellular metabolism such as isocitrate dehydrogenase (IDH) and mitochondrial-D-lactate dehydrogenase (D-LDHm) were also found to be differentially regulated. IDH plays a key role in TCA cycle and isocitrate-alpha-ketoglutarate cycle while D-LDHm aids in the elimination of toxic metabolite methylglyoxal, involved in protein degradation. These findings will enhance our efforts towards understanding why certain CHO cell lines exhibit enhanced performance and perhaps provide future cell engineering targets.

KEYWORDS
adhesion, CHO, fold change analysis, pathway analysis, proteomics

1 | INTRODUCTION

Following establishment of the first Chinese hamster ovary (CHO) cell lines in 1957 by Dr. Theodore Puck, several derived lineages of CHO cells, such as CHO-K1, CHO-DG44, CHOK1SV, and others have enjoyed widespread usage for production (Dhara et al., 2018) of the majority of biotherapeutics manufacturing, including more than 160 commercial recombinant products (Dahodwala & Sharfstein, 2017). Some of the key features behind the success of CHO cells are their ability to grow to high density as suspension cultures with high viabilities in large-scale bioreactors while exhibiting human-compatible posttranslational modifications. Yields for monoclonal antibodies biotherapeutics produced by CHO can reach up to 1–10 g/L range (Kildegaard et al., 2013).

There is a continuing desire to understand the most favorable aspects of these cell lines with the eventual goal of improving recombinant protein production (Kelley, 2020). Due to the high plasticity of CHO cells, the derived host cell lineages and recombinant clones may possess distinct genotypic and phenotypic signatures which may alter their capacity for scale-up and yield.

For characterization, various Omics' tools have been employed in CHO cells (Farrell et al., 2014; Stolfa et al., 2018), across different CHO hosts and producer cell lines. For example, Doolan et al. (2013) used gene expression analysis to identify correlations between transcripts expression levels and cellular growth rates. Likewise, Singh et al. (2018) used RNA-seq studies to characterize and quantitatively categorize several CHO cell lines.

Following initial whole genome wide proteomic analysis of Chinese Hamster tissues and CHO cells performed by our group and others (Baycin-Hizal et al., 2013), multiple proteomics studies have emerged more recently to characterize proteomic signatures of high producing CHO cell clones, host cell protein impurities, secreted proteins, and other pathways important in biotherapeutics protein production and growth (Heffner et al., 2020). For example, Schelletter et al. (2019) used a combination of label-free and stable isotope labeling by amino acids in cell culture-based phosphoproteomic approach to elucidate protein expression differences related to stress response and cellular homeostasis. Blondeel et al. (2016) used 2D-DIGE proteomics to identify changes in pathways related to anaplerotic tricarboxylic acid (TCA)-replenishment, NADH/NADPH replenishment and redox modulation, while Müller et al. (2017) studied CHO cell response 25 h after butyrate treatment using a label-free electroSpray Ionization-Mass Spectrometry quantification. Sommeregger et al. (2016) observed that the product itself has a large impact on the proteome of the cell. While proteomic data sets can provide a clear depth of information about bioproduction platforms, it can also lead to a deeper understanding and greater insights into cellular processes by integration with multiple omics technologies including transcriptomics, glycomics, and others.

For this study, we compared two CHO host cell lines and two clones from each host following transfection with an antibody gene. We observed that the clones H1C1 and H1C2, obtained from the in-house derived H1, had higher titer (greater than 6-fold) and specific productivity (Qp greater than 3.5-fold), despite lower copy numbers for the heavy and light chains (HCs and LCs) in comparison to commercial recombinant clones. This prompted us to undertake a tandem mass tag (TMT)-proteomic study to leverage the power of proteomics to investigate cellular changes that could lead to different cellular performances such as growth and productivity.

Based on our proteomic data, we observed significant differential regulation in pathways including cell adhesion or aggregation. In the context of bioprocesses, cell aggregation hinders accurate cell growth determination and negatively affects cell growth and productivity by inhibiting efficient mass transfer in the cell culture medium. It also poses challenges during scale-up in biomanufacturing processes, prompting the use of anticlumping agents such as suramin, to reduce cell clumping. Furthermore, this aggregation can be exacerbated by the presence of cellular DNA released from decaying and dead cells, enhancing cell–cell contact. Hence, it is of importance to limit cell aggregation in biomanufacturing processes, to better control growth, metabolism and productivity of CHO cells.

Apart from pathways associated with physical characteristics, we also observed other proteomic differences, including cellular metabolism. Indeed, one of the critical means to improve cellular performance is by altering cellular metabolism, either by modifying the culture medium through the usage of additives such as growth factors, lipids, hydrolysates (Jenkins et al., 1994; Kumar et al., 2020), or through genetic manipulation to eliminate toxic metabolites. Alternate strategies include using cell line engineering methods to overexpress glutamine transferase to lower ammonia production or modifying other key components of glycolysis and TCA cycle that can lead to enhancements in growth and titer as high as threefold (Richelle & Lewis, 2017).

Given the influence of cellular metabolism on recombinant protein productivity, we attempted to find specific differences in metabolism between the two hosts, H1 and H2, as well as representative clones H1C1 and H1C2 and H2C1 and H2C2. We observed differential regulation in protein levels across several pathways including TCA cycle and methylglyoxal pathway. These findings will assist the community efforts to further understand CHO physiological characteristics and metabolism to increase their performance characteristics in the production of valuable biologics.

2 | METHODS

2.1 | Cell culture

An in-house suspension CHO host cell line (H1) and a commercial CHO cell line (H2) were used for the study. Both the hosts were transfected with plasmid containing for the protein of interest and subjected to single cell cloning as adopted in Huhn et al. to obtain two clones each from the respective host (H1C1, H1C2, H2C1, H2C2) (Huhn et al., 2019). The cells were cultured in 125 ml shake flasks in their respective media, with or without L-glutamine, in a shaker incubator at 36.5°C at 140 rpm and 5% CO_2. Cells were passaged at a seeding density of $0.2–0.5 \times 10^6$ viable cells/ml every 2–3 days depending on doubling time and passage duration to target $1.5–3.0 \times 10^6$ viable cells/ml on passage day in a shaking incubator.

2.2 | Fed batch cultivation

To quantify and assess differences in productivity, the cells were cultured in a fed-batch mode by culturing in the respective media. The cells were passaged for >3 passages before N-1 inoculation. For inoculating production cultures (N), cells from passaging cultures were seeded at $0.2–0.5 \times 10^6$ viable cells/ml, depending on clone doubling time and N-1 passage duration, in chemically defined Fed Batch Production Media. Glucose and lactate levels were measured everyday using the RANDOX RX imola chemistry analyzer (Crumlin). Cell density and viability were using a Beckman Coulter ViCELL cell counter (Beckman Coulter). One milliliter of sample was harvested from production cultures for product quality analysis. Samples were collected via centrifugation and the supernatant was filtered and submitted to Analytics for Pro-A Titer, determined by a Protein-A ultra performance liquid chromatography (UPLC).

2.3 | Adhesion assay

Approximately 20,000 cells were seeded in replicates into 96-well plates coated with extracellular matrix (ECM) substrate (Biocoat; Corning) and placed in a static incubator set to 37°C. Cells were then washed four times with prewarmed media and gentle trituration using a multichannel pipette following a 0.5-, 1-, and 2-h incubation period. Plates were returned to incubator in between wash steps. Following the last wash, cells were incubated with 3-(4,5-dimethylthiazol-2-yl)-2,5-diphenyl tetrazolium bromide (MTT) according to manufacturer's instructions (Abcam; Cat: ab211091). Briefly, plates were incubated at 37°C with MTT reagent for 3 h, the media was gently aspirated from each well, and MTT solubilizing solution was then added to each well. Following gentle shaking in an orbital shaker for 10 min, plates were read using a plate reader at 590 nm. The average of eight replicate wells was summed, subtracted from background, and is represented as a fraction of unwashed control. Experiments were performed in biological replicates.

2.4 | Proteomics sample preparation

Three million cells were obtained as pellets, washed with ice-cold phosphate buffered saline, snap frozen on dry ice and stored at −80°C for proteomic analysis. These pellets were later thawed and subjected to cell lysis by resuspension in a 2% solution of sodium dodecyl sulfate (SDS; Thermo Fisher Scientific; Cat No. 24730020) containing 0.1 mM phenylmethylsulfonyl fluoride (Sigma [SAFC]; Cat No. 10837091001) and 1 mM ethylenediaminetetraacetic acid (Sigma [SAFC]; Cat No. 03620) at pH 7–8. The samples were then subjected to sonication in bursts of 30 s at 20% amplitude followed by a 45 s pause (three cycles). Resultant protein extract concentration was measured by bicinchoninic acid (BCA) protein assay kit (Thermo Fisher Scientific; Cat No. 23225) and the samples were quality checked on SDS-polyacrylamide gel electrophoresis and stained using Protea Biosciences' SuperBlue Ultra™ Coomassie Stain to ensure no protein degradation (Supporting Information: Figure S1).

2.5 | TMT proteomics

For the TMT 10-plex, hosts H1 and H2 were analyzed in duplicate along with clones H1C2 and H2C2 in duplicate. Clones H1C1 and H2C1 were analyzed as singlicates, due to limitations in TMT 10-plex protocol sample size. Protein extracts were reduced with 10 µl of 200 mM tris(2-carboxyethyl)phosphine, alkylated with 10 µl of 375 mM iodoacetamide in the dark for 30 min, and TCA/acetone precipitated (100 µg). Protein pellets were resolubilized in 100 µl of 100 mM triethyl ammonium bicarbonate (TEAB) and were digested overnight at 37°C by adding 10 µg of Trypsin/LysC mixture (V5071; Promega) in 100 mM TEAB. Individual samples (100 µg) were labeled with a unique isobaric mass tag reagent (TMT 10-plex; Thermo Fisher Scientific) according to manufacturer's instructions. Both pairing and labeling order of TMT reagent and peptide sample were randomized. Briefly, the TMT reagents (0.8 µg vials) were allowed to come to room temperature before adding 41 µl of anhydrous acetonitrile, then vortexed and centrifuged. The entire TMT reagent vial was added to the 100 µg peptide sample and reacted at room temperature for 1 h. Five percent of hydroxylamine (8 µl) was then added to quench the reaction. All TMT labeled samples were combined and vacuum centrifuged to dryness removing the entire liquid. The combined samples of TMT labeled peptides were resuspended in 2 ml of 10 mM TEAB and separated into 84 fractions at 250 µl/min using a 0%–90% acetonitrile gradient in 10 mM TEAB on a 150 mm × 2.1 mm ID Waters Xbridge 5 µm C18 using an Agilent 1200 capillary high-performance liquid chromatography in normal flow mode and Agilent 1260 micro-fraction collector. The 84 fractions were concatenated into 24 fractions by combining all odd rows of each column 1 through 12 into 12 fractions and all even rows of each column into another 12 fractions.

The peptide fractions were resuspended in 20 µl 2% acetonitrile in 0.1% formic acid and 0.9 µg (25%) was loaded onto a C18 trap (S-10 µM, 120 Å, 75 µm × 2 cm; YMC) and subsequently separated on an in-house packed PicoFrit column (75 µm × 200 mm, 15 µm, ±1 µm tip; New Objective) with C18 phase (ReproSil-Pur C18-AQ, 3 µm, 120 Å, https://dr-maisch.com) using 2%–90% acetonitrile gradient at 300 nl/min over 120 min on a EasyLC nanoLC 1000 (Thermo Fisher Scientific). Eluting peptides were sprayed at 2.0 kV directly into a Q-Exactive HF (QE Plus; Thermo Fisher Scientific) mass spectrometer. Survey scans (full ms) were acquired from 350 to 1800 m/z with data-dependent monitoring of up to 15 peptide masses (precursor ions), each individually isolated in a 1.2 Da window and fragmented using HCD activation collision energy 32 and 15 s dynamic exclusion, with a scan range of 120–2000 m/z. Precursor and fragment ions were analyzed at resolutions 120,000 and 45,000, respectively, with automatic gain control target values at $3 × 10^6$ with 60 ms maximum injection time (IT) and $1 × 10^5$ with 150 ms maximum IT, respectively.

2.6 | Data analysis

Isotopically resolved masses in precursor (MS) and fragmentation (MS/MS) spectra were extracted from raw MS data using spectrum selector with recalibration in Proteome Discoverer (PD) software (v2.1; Thermo Fisher Scientific) and searched using Mascot (2.5.1; www.matrixscience.com) against a custom Chinese Hamster protein database (created February 6, 2019, containing 38,529 sequences). The following criteria were set for all database searches: (1) All species in database; (2) Trypsin as the enzyme; (3) Allowing two missed cleavage; (4) N-terminal TMT6plex and cysteine carbamido-methylation as fixed modifications; (5) Lysine TMT6plex, methionine oxidation, serine, threonine and tyrosine phosphorylation, asparagine and glutamine deamidation as variable modifications; (6) Precursor and fragment ion tolerance was set to 5 ppm and 0.03 Da, respectively. Peptide identifications from Mascot searches were filtered at 1% false discovery rate (FDR) confidence threshold, based

on a concatenated decoy database search, using the Proteome Discoverer. Proteome Discoverer uses only the peptide identifications with the highest Mascot score for the same peptide matched spectrum from the different extraction methods. The protein intensities were reported as S/N of each peptide and relative protein comparisons were calculated using the peptide grouping in Proteome Discoverer. Quan value correction factors were used and a coisolation threshold of 30 was used. Peptide abundances were normalized against a custom set of histone proteins (three sequences, created June 25, 2019) to ensure that there was no experimental bias in protein quantification that was dependent on total amount of nuclear proteins. An overview of the experimental and data analysis pipeline can be found in Figure 1.

3 | RESULTS

3.1 | Cell culture

Antibody expressing clones from both hosts (H1C1, H1C2, H2C1, and H2C2) were cultured for 10 days in a fed-batch process. Total titer (g/L) produced by the clones was quantified on Day 10 using a Protein-A UPLC and plotted in Figure 2a. Specific productivity, Qp (pg/cell/day) was calculated, using Integral Viable Cell Density (Supporting Information: Figure S2A) and plotted in Figure 2b. Peak VCD plot can be found in Supporting Information: Figure S2B. It was observed that clones H1C1 and H1C2 had higher titers (~6.8 times) and a higher Qp (~2.3 times), despite lower copy number for the HCs (HC1, HC2) and LCs (LC1, LC2) (Supporting Information: Figure S2C,D). Furthermore, upon comparing the host cells H1 and H2, we observed significant clumping of H2 cells under the microscope (Figure 2c) and the formation of a ring of dead cells and debris on the surface of the flask (Supporting Information:

Figure S3G). Using fibronectin as the matrix, a cell adhesion assay was performed to further investigate any differences in adhesion between to two host cell lines (H1 and H2) using an adherent cell line as a control. Cells from host H2 were found to exhibit stronger adhesion properties as indicated by percent adherent cells after an hour of plating in comparison to H1 cells (Figure 2d).

3.2 | Fold change analysis

Using three million cells, protein extracts were prepared, labeled with a unique isobaric mass reagent, and subjected to TMT-10plex based proteomics analysis (Figure 1). As a measure of differential expression, fold-changes were determined using abundance ratios from the TMT proteomics data across host and clonal cell lines. By observing differences in fold-changes across samples, differential regulation of proteins and pathways can be identified. Based on a protein FDR of 1% or less, we categorized proteins with fold-change ratio values greater than 2.0 as being upregulated while those with values below 0.5 were considered to be downregulated. This analysis was performed between the two hosts (H1 and H2) and between the two clones from the two different hosts (H1C1, H1C2, H2C1, and H2C2). $\log_2$fold change ratios were plotted against $\log_{10}$ p values as volcano plots to provide quick visualization of statistically significant global protein regulation differences while also identifying highly differentially regulated proteins (Supporting Information: Figure S4). Based on these plots, we observed specific patterns of proteins and groups of proteins that exhibited differential regulation between the two hosts and/or clones.

Interestingly, an analysis of the volcano plots of fold-change values obtained by comparing hosts (H1 vs. H2) (Figure 3a) and two clones (H1C1 vs. H2C1, H1C2 vs. H2C2) indicated a differential regulation of several proteins involved in pathways related to cell
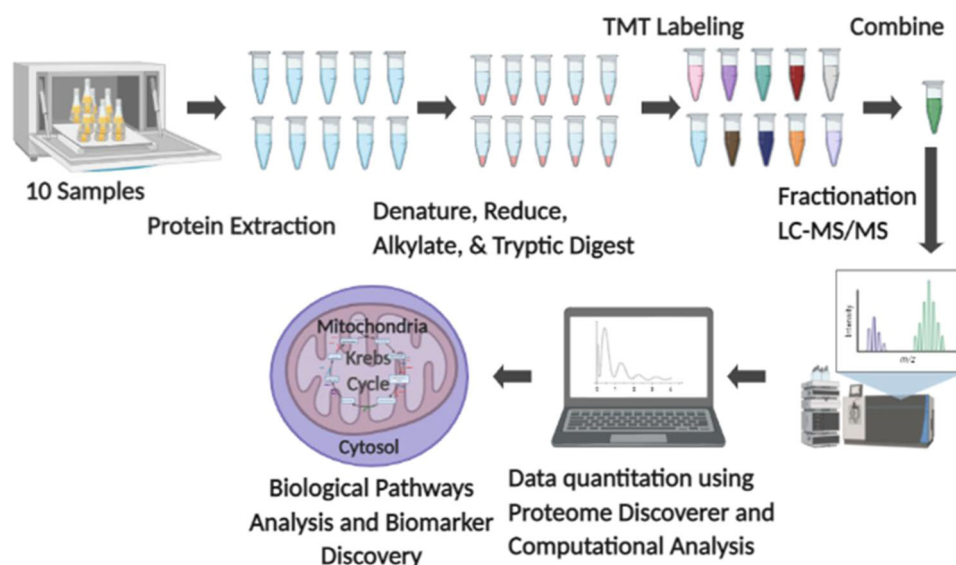

FIGURE 1 Schematic of study design and proteomics analysis pipeline.
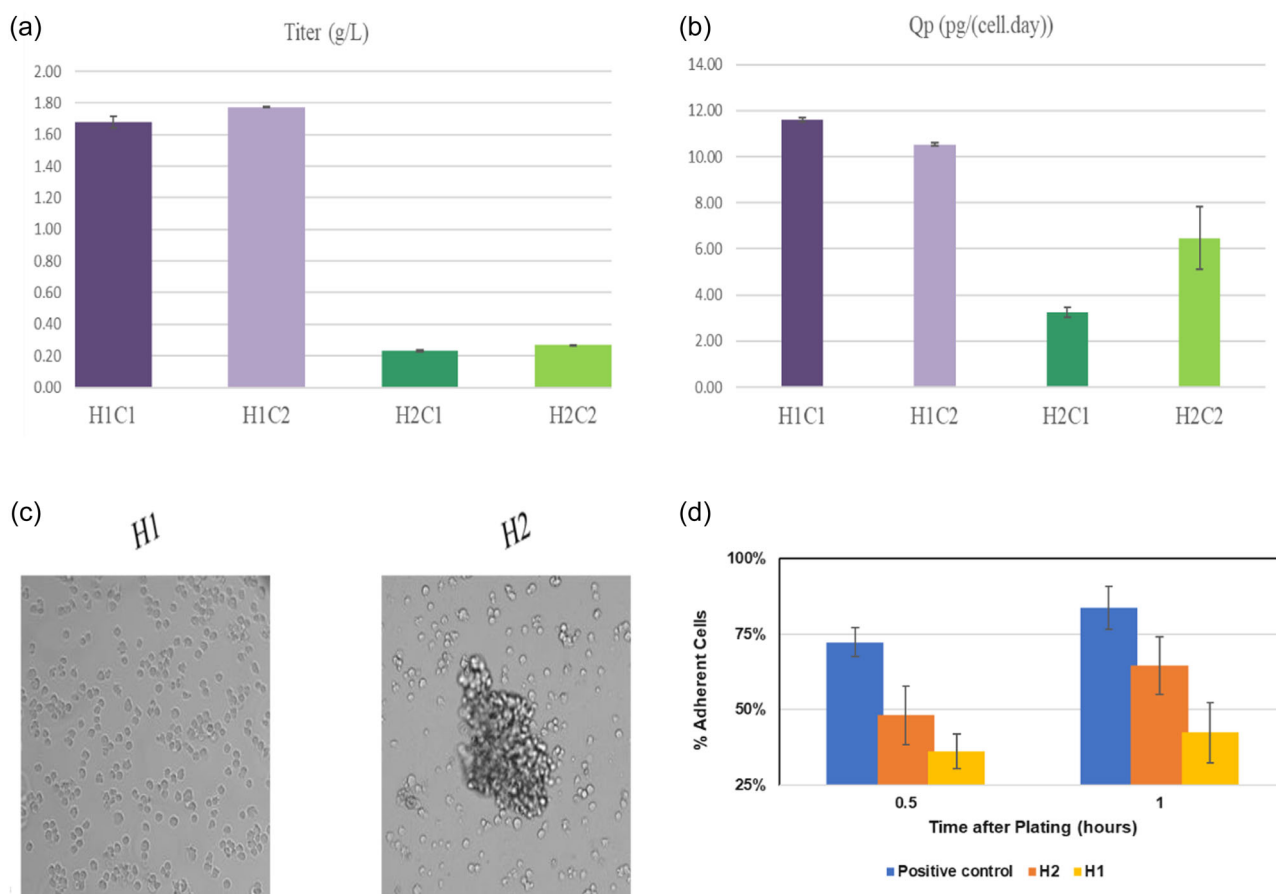
FIGURE 2 Cell culture observations (cell aggregation and productivity) of host (H1, H2) and clones (H1C1, H1C2, H2C1, H2C2). (a) Titer (g/L) for clones (C1, C2) of H1 and H2; (b) specific productivity Qp (pg/cell/day) for clones (C1, C2) of H1 and H2; (c) host CHO cells H1 and H2 viewed under the microscope; (d) fibronectin based adherent cell assay, to check for cellular adhesion to matrix.

adhesion. In particular, podoplanin, a mucin-type transmembrane glycoprotein known to be involved in cell adhesion, was upregulated the highest, in H1, at a factor of 14, compared to H2 (Supporting Information: Figure S3A). This led us to check for differential regulation of other proteins involved in cell adhesion. As indicated in Figure 3a–c, a significant number of proteins involved in cell adhesion were differentially regulated, mostly downregulated, in H1. These differentially regulated proteins include layilin, fibronectin, tensin-1, paxillin (Pax), and others, apart from podoplanin. This downregulation was also retained in the resulting clones H1C1 and H1C2, with the specific levels of differential regulation of these proteins described in Supporting Information: Figure S3A–F.

Cell adhesion can be a challenging parameter to evaluate experimentally, especially in suspension cultures. Empirical evidence was indicated by the formation of a ring of cell debris on the surface of the flask following cultivation of H2 cells (Figure 2c and Supporting Information: Figure S3D), providing a physical indication that host H1 may have been less adhesive. In addition, we performed a cell adhesion assay, using a matrix composed of fibronectin. By comparing each host to an in-house adherent cell line as a positive control, cells from H1 were observed to be less adherent to the fibronectin surface than those from H2 (Figure 2d).

In addition to pathways such as cellular adhesion, we also examined differentially regulated proteins involving cellular metabolism. For example, cytoplasmic isocitrate dehydrogenase (IDH1), involved in the isocitrate/α-ketoglutarate (IC/AKG) shuttle between the cytosol and the mitochondria was observed to be downregulated with a 0.43-fold change ratio in H1 versus H2 and also to 0.35- and 0.45-fold in the respective clonal comparisons. IDH1 converts cytosolic IC to AKG with the production of NADPH. Given the role of IDH1 in this shuttle, we further examined other proteins involved in this and other associated shuttles, TCA cycle activity, and mitochondrial function as shown in Figure 4. Interestingly, the tricarboxylate transport protein (SLC25A1), which transports citrate from the mitochondria, and the mitochondrial 2-oxoglutarate/malate carrier protein, that transports AKG back into the mitochondria, were upregulated and moderately downregulated, respectively. Also, while one of the mitochondrial homologs of IDH, IDH2, exhibited limited changes in expression, the other mitochondrial form, IDH3, was upregulated in the clonal comparisons (greater than 1.5-fold). Other mitochondrial proteins involved in the TCA cycle that were also differentially expressed include the mitochondrial NAD(P) transhydrogenase (NNT), that acts as a proton leakage pump, which was moderately upregulated in host H1 at 1.36-fold.
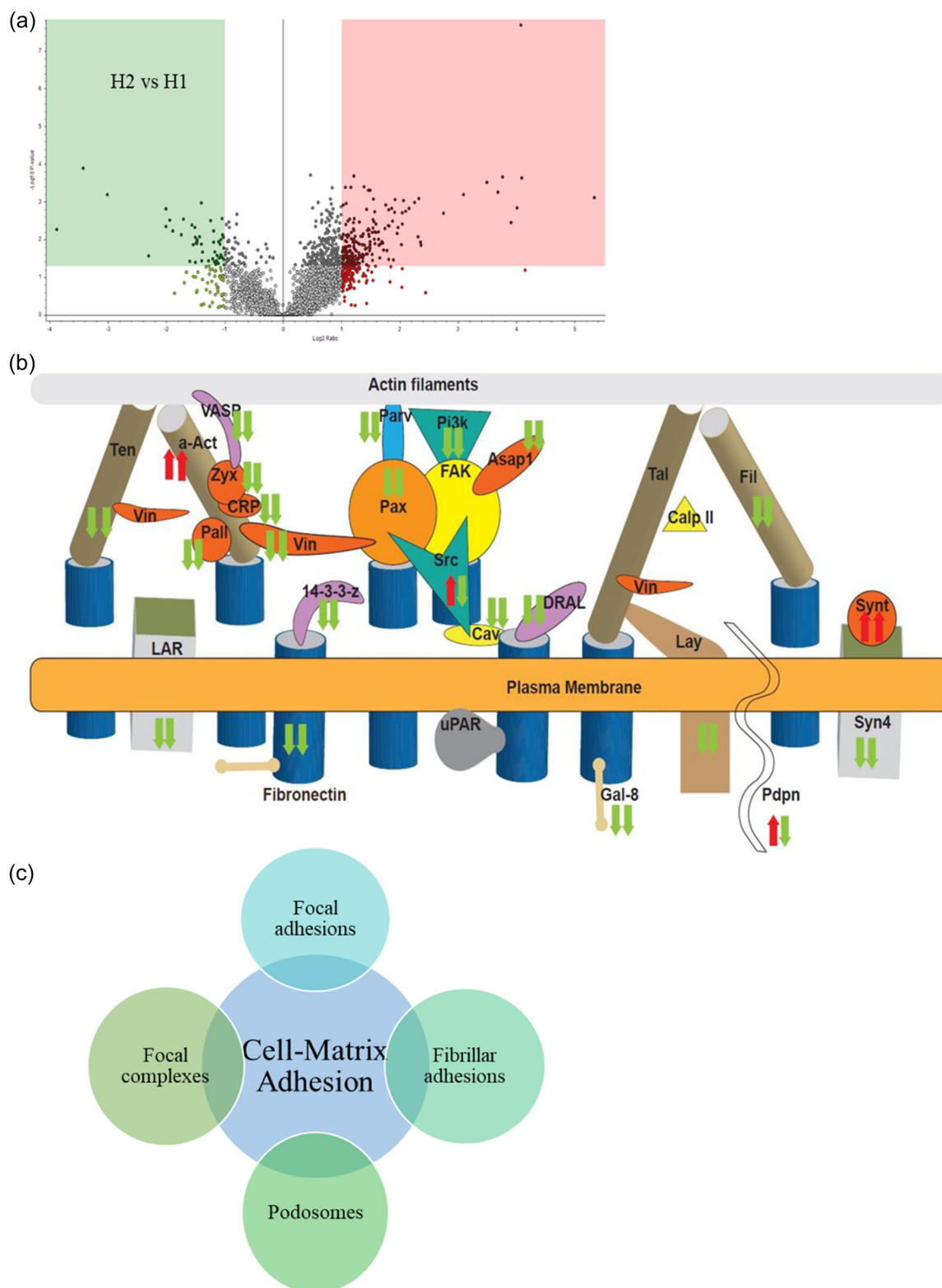
FIGURE 3 Overview of the different types of cell–matrix adhesions along with the differential regulation of proteins in the cell lines. (a) Volcano plot of $\log_{10}$ p-value versus $\log_2$ ratio of H2 versus H1. Significant proteins with Log FC > 1.0 or <−1.0 can be observed in the shaded boxes (red—upregulation; green—downregulation); (b) first arrow—up (red) or down (green) regulation in proteome data; second arrow—effect on adhesion pathway (up—red, down—green); (c) schematic of different types of cell–matrix adhesions.
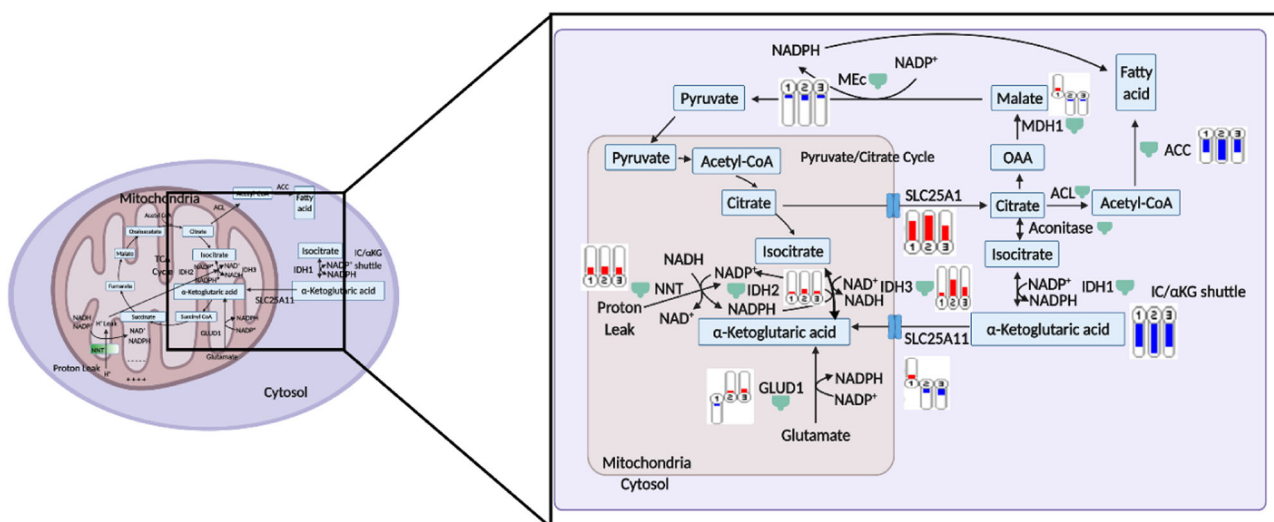
FIGURE 4 Overview of different IDH reactions and pathway in mammalian cells. ![enzyme] indicates an enzyme. Thermometers indicate fold change ratios: 1: H1 versus H2; 2: H1C1 versus H2C1; 3: H1C2 versus H2C2. IDH, isocitrate dehydrogenase.

Other proteins involved in metabolism including mitochondrial-D-lactate dehydrogenase (D-LDHm) and cytochrome *c* (CYT*c*) were also observed to be upregulated, including by more than two fold for D-LDHm in the host H1 versus H2 and equally high for the related clonal comparisons. The D-LDHm is responsible for the conversion of D-Lactate into pyruvate. While D-lactate is present in lower amounts compared to L-lactate, the metabolite is generated as a result of metabolic degradation of the potentially toxic methyl-glyoxal (MGO) metabolism in mammalian cells. Importantly, MGO, a 2-oxoaldehyde, is a toxic metabolic observed to be damaging to mammalian cell growth. Thus, elimination of this toxic metabolite could potentially aid in better performance of the clones from and cells of the host H1.

3.3 | Pathway analysis

While fold-change analyses highlight differentially expressed proteins, they, however, lack a network level description of the changes that may be occurring in the cell. Pathway analyses can bridge this gap by identifying clusters of protein groups that are differentially expressed and thus enriched. These analyses were carried out through Metascape (Zhou et al., 2019), in which lists of differentially regulated significant (*p* < 0.1) genes were used as inputs to identify enriched pathways. Metascape can facilitate Omics' data analyses by integrating more than 40 knowledgebases and hence offering a multilevel analysis of systems-level data.

From Metascape, we obtained different lists of enriched pathways for the varied hosts and clonal comparisons. Upon evaluation of the enriched host protein pathways, it was observed that apart from cell adhesion and aggregation, previously discussed in the Fold-change analysis section, multiple pathways involved in lipid and cholesterol metabolism, including sterol and isoprenoid biosynthesis,

were also downregulated in host H1 (Supporting Information: Table ST1). Genes included in the pathway such as mevalonate diphosphate decarboxylase, 3-hydroxy-3-methylglutaryl-CoA reductase (Hmgcr), cytoplasmic 3-hydroxy-3-methylglutaryl-CoA synthase (Hmgcs) were found to be downregulated to at least 0.3-fold expression levels in host H1, compared to H2. Similar trends were also observed in clonal comparisons. In addition, the lowered expression of these proteins also resulted in the downregulation of the related mevalonate pathway, which produces C-5 isoprenoids and is involved in terpenoid backbone synthesis. Interestingly, downregulation was also observed in protein catabolic processes, of which IDH1 is a member, as noted in the fold-change section. In addition to IDH1, expression of several proteins was reduced in this pathway, including Hmgcr, histone acetyltransferase 300 (Ep300) and others (Supporting Information: Table ST1).

4 | DISCUSSION

Following analysis of significantly differentially regulated proteins, we observed groups of proteins associated with specific pathways, including cell adhesion, that were differentially regulated. Cell adhesion is a tightly regulated process that can have a significant impact on CHO biomanufacturing. Studies have shown that cell aggregation decreases specific growth rates while also increasing death rates for cells in culture due to its detrimental effects on efficient mass transfer (Chiquet-Ehrismann, 1995; Renner et al., 1993). Indeed, in the current study, H2 host cells tended to adhere to surfaces and to each other (Figure 2C, Supporting Information: Figure S3G) more readily than the other host H1. This adhesion of cells to surfaces and each other can be driven by multiple factors including in some cases proteins of the ECM. Interactions with the ECM affect cells in multiple ways that can trigger numerous

responses. The ECM also acts as a scaffold, impacting basic cellular processes such as proliferation and cell death (Geiger et al., 2001).

ECM adhesions are primarily characterized by focal adhesions along with fibrillar adhesions, podosomes, and focal complexes. Importantly, the majority of these were downregulated in host H1 in comparison to host H2. This difference in expression of ECM adhesions was also evident in the clones H1C1 and H1C2. ECM adhesions are primarily mediated by integrins, which were also observed to be downregulated along with podoplanin in H1, that interact with the actin cytoskeleton of the cell interior. These adhesions are anchored by ligands such as vitronectin, fibronectin, and so forth. Indeed, both fibronectin and vitronectin were found to be downregulated in host H1 versus H2 comparisons, as noted in Supporting Information: Figure S3B.

Of the different types of ECM adhesions, focal adhesions, comprised of flat, elongated structures located near the cellular periphery with an area of several square microns in magnitude (Geiger et al., 2001), bind actin microfilaments, and thus form strong adhesions through a plaque of proteins (Figure 3c). Proteins such as vinculin (Vin), Pax, and talin comprise a few examples of such proteins. Talins transition integrins from an inactive to an active state by simultaneously binding to their cytoplasmic domain and to filamentous actin, Vin, and the actin cross-linking protein α-actinin (Parsons et al., 2010). The observed downregulation of Vin and Pax (Figure 3b and Supporting Information: Figure S3B,D,F) in H1 suggests that focal adhesion interactions were also reduced in H1.

Multiple ligands can serve as binding partners for fibronectin and be involved in the cell adhesion process through formation of fibrillar structures, which comprise yet another mechanism for ECM adhesion (Figure 3c). These dot-like structures are primarily composed of extracellular fibronectin fibrils, fibronectin receptor, and proteins such as tensin, which were all downregulated (Figure 3b and Supporting Information: Figure S3A–F). Fibronectin, which was downregulated to 0.32-fold expression in H1 compared to that of H2, binds with multiple ligands such as podoplanin, galectin-8, syndecan-4, and so forth. Podoplanin, which interacts with galectin-8 (Cueni & Detmar, 2009) and spans the plasma membrane, was upregulated the highest, at a factor greater than 14 for host comparisons (H1 vs. H2) and greater than 3 for clonal comparisons (H1C1 vs. H2C1, H1C2 vs. H2C2). Though the exact function is unknown, podoplanin is a well-conserved mucin-type trans-membrane glycoprotein with various roles including involvement in cell adhesion in association with galectin-8, a subclass of tandem-repeat type galectin known to interact with cell-surface integrins (Astarita et al., 2012), and so forth. Interestingly, podoplanin has been shown to function as an antiadhesion molecule in the absence of C–C motif chemokine 21 (CCL21) (Cho et al., 2017; Tejchman et al., 2017; Ugorski et al., 2016) or as a proadhesion molecule in association with C-type lectin receptor2 (CLEC2) (Kunita et al., 2007; Suzuki-Inoue et al., 2007). The absence of detected CCL21 along with down-regulation of CLEC2 and galectin-8 (Supporting Information: Figure S3A–F) prompted us to propose that the antiadhesion activity of podoplanin may play a role in the reduced cell adhesion properties

of host H1. We also observed that other protein partners of fibronectin such as syndecan-4, leukocyte antigen receptor, layilin were also downregulated, indicating to an overall downregulation of fibrillar adhesions.

While fibrillar adhesions make up a second major class of cellular adhesions, a third type of ECM adhesions consist of podosomes (Figure 3c). These cylindrical structures are made up of proteins such as Vin and Pax which were downregulated and dynamin (Figure 3b), suggesting a similar downregulation of ECM adhesions through podosomes. The final class of ECM adhesions are made up of focal complexes, that could either serve as precursors of focal adhesions or be associated with cellular migration. Component proteins such as Ras-related C3 botulinum toxin substrate 1 were found to be downregulated, thus likely also downregulating the formation of focal complexes.

In total, we observed that the aforementioned types of cell–matrix adhesions were downregulated in the H1 versus H2 cell line comparison, consistent with the difference in phenotype observed for the two cell lines in culture. Since cell adhesion is likely to be problematic for biomanufacturing, lowered cellular adhesion can be considered as one of the early markers of undesirable cell performance characteristics to avoid in choosing a host cell line. Indeed, clones from host H1 outperformed those from host H2, in terms of both titer and productivity of a monoclonal antibody (Figure 2a,b). In the future, probing for cells with these pathways downregulated or else deliberately manipulating them could acceler-ate the often-time-consuming process of early host cell line selection for bioproduction, leading to a richer pool of cell hosts from which to choose the optimal performing clones, in terms of other desirable properties of importance for large scale biomanufacturing.

Upon examining other differentially regulated proteins involved in metabolism, we noted that proteins including IDH1, D-LDHm, CYTc, and others were differentially regulated. Of these, IDH1 plays an important role in glucose metabolism, as part of the IC/AKG shuttle (Figure 4) and was observed to be downregulated to 0.43-fold expression in H1 versus H2. IDH1 acts on cytosolic IC, which can be transported by SLC25A1 (found to be upregulated by greater than 1.3-fold in H1 and associated clones), and converts it into AKG along with the production of NADPH. Among other dispositions, the resulting AKG can then be transported back into the mitochondria by mitochondrial 2-oxoglutarate/malate carrier protein and converted into pyruvate through the malate/pyruvate shuttle (Figure 4). Previous studies have established energy consumption by the IC/ AKG shuttle while producing NADPH (Guay et al., 2013).

Downregulation of IDH1 could lead to decreased production of cytosolic NADPH which, if not compensated by the pentose phosphate pathway (PPP), can potentially lead to a reduced cytosolic NADPH/NADP$^+$ ratio, while increasing cytosolic IC and NADP$^+$ concentrations. Indeed, enhanced NADP$^+$ levels may be advanta-geous to CHO cells if the other pathways can make up for the loss of NADPH production via this reaction. The decrease in NADPH production from the IC/AKG cycle may be compensated by its generation in the PPP, given that glucose, which feeds into PPP, was

fed as the predominant carbon source. Meanwhile, the cytosolic citrate can be converted to pyruvate and then recycled back into the mitochondria through the citrate–malate cycle (Figure 4) or converted to other cellular products such as acetyl-Co-A. Once in mitochondria, the citrate produced from pyruvate can be shuttled back to the cytosol via the upregulated SLC25A1. In addition, IDH3, which facilitates the conversion of IC to AKG in the mitochondria along with the conversion of NAD^+ to NADH, was observed to be upregulated by greater than 1.5-fold in the clonal comparisons (H1C1 vs. H2C1; H1C2 vs. H2C2). This production of NADH, a precursor for ATP generation through oxidative phosphorylation, will be useful for providing energy to drive other cellular activities, suggesting that mitochondrial NADH production (from IDH3) is preferred at the expense of cytosolic NADPH generation (from IDH1) in these CHO cells. Also moderately upregulated NNT can use the excess NADH in the cell, converting it to NAD^+, along with the production of NADPH, which is used for anabolic processes in the mitochondria (Figure 4). Overall, mitochondrial NADH may be a more valuable currency to cells than cytosolic NADPH, which is somewhat surprising since NADPH is important to growth, biosynthesis and activities of glutathione and thioredoxin reductases.

Furthermore, IDH1 controls the concentration of cytosolic AKG, which acts as a co-factor for BCAT1, in the catabolism of branched chain amino acids (BCAAs). The first step of this pathway involves the conversion of the α-amino acids such as leucine, isoleucine, and valine into their α-keto-acid form. Hence, a downregulation in the IDH1 gene would lead to decreased availability of cytosolic AKG and thus to a downregulation in the BCAA catabolism, led by BCAT1 (Tönjes et al., 2013). Indeed, we did observe a downregulation in proteins involved in catabolism, for the host cells H1 from our gene ontology (GO) and kyoto encyclopedia of genes and genomes (KEGG) pathway analyses using Metascape. Interestingly, prior studies in CHO and *Saccharomyces cerevisiae* (Kazemi Seresht et al., 2013; Ley et al., 2015) have elucidated the possible adaptations that cells undergo to increase their specific heterologous protein productivity, specifically in reducing amino acid catabolism, such that amino acids can instead contribute to the production of the heterologous proteins. Hence, IDH1 knockdown in cells from host H1 may rewire their cytoplasmic metabolism, yielding clones with the potential for higher specific protein productivities.

IDH1 has also been found to be involved in lipid and cholesterol biosynthesis, through an increased consumption of acetyl-Co-A and malonyl-Co-A. Transgenic mice with elevated IDH1 expression were found to be obese, with hyperlipidemia and a fatty liver (Koh et al., 2004). Lipid biosynthesis requires a high NADPH/$NADP^+$ ratio, with NADPH acting as an essential cofactor in fatty acid generation. As a key producer of NADPH, downregulation of IDH1 may correlate with a change in lipid synthesis. This is further supported by the GO and KEGG pathway analysis, wherein cholesterol metabolism, and sterol and isoprenoid biosynthetic processes were found to be downregulated in host H1 compared to H2. The mevalonate pathway, resulting in the production of C5 isoprenoids from acetyl-Co-A, was also found to be downregulated in H1. Thus, the host H1 cells may have shifted their metabolism through downregulation of IDH1, to limit fatty acid synthesis, resulting in "leaner" host mammalian cells. Interestingly, our group has also observed epigenetic differences in the mevalonate pathway between the cell lines under investigation (Chang et al., 2022), consistent with the proteomic findings of this study.

Another metabolic enzyme, D-LDHm was found to be upregulated, has been previously found in mammalian cells (Flick & Konieczny, 2002), and is known to be involved in catabolism of D-Lactate to pyruvate. Although L-lactate is the predominant form found in cells, D-lactate is produced in small quantities (Talasniemi et al., 2008) as a result of MGO metabolism (Ewaschuk et al., 2005; Uribarri et al., 1998). MGO is a protein and nucleic acid modifying agent, synthesized by actively growing cells as a result of spontaneous phosphate elimination, and MGO synthase arising from intermediates during glycolysis (Figure 5). MGO can also be produced as a result of lipid, L-threonine and L-glycine catabolism. MGO is a cytotoxic compound proven to be detrimental to cultured cells including an association with cell death (Kingkeohoi & Chaplen,
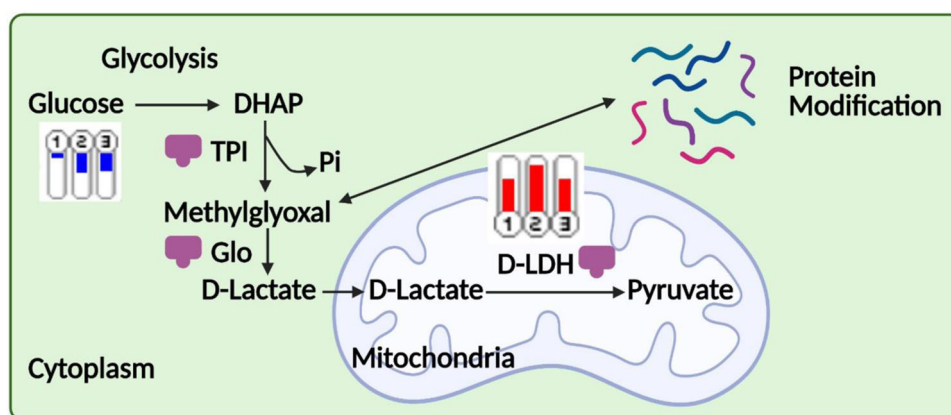

FIGURE 5 Overview of pathway and function of D-LDHm in mammalian cells. ▇ indicates an enzyme. Thermometers indicate fold change ratios: 1: H1 versus H2; 2: H1C1 versus H2C1; 3: H1C2 versus H2C2. D-LDHm, mitochondrial-D-lactate dehydrogenase.

2005). Previously, Chaplen et al. (1996) observed that MGO negatively affected the viability of actively growing CHO cells, and also depended on media composition. MGO can be converted to D-lactate through the glyoxalase system (Glo1 and Glo2 in Figure 5). This synthesized D-lactate can then be localized to the mitochondria (De Bari et al., 2002), and, in turn, converted to pyruvate through D-LDHm. Previous studies in plants have confirmed the role of D-LDHm in MGO detoxification (Welchen et al., 2016). Welchen et al. also show that overexpression of CYTc, in conjunction with D-LDHm, lead to increased tolerance of D-lactate and MGO in plants. Interestingly, CYT*c* was also upregulated by 2.4-fold in clone H1C2 versus H2C2. CYTc, when released from mitochondria, has been known to have apoptotic activity. This apoptotic activity occurs in combination with Bcl2 proteins, which were not found to be differentially regulated in our proteomics data. Chandra et al. (2002) also suggest that a simple upregulation of CYTc alone is insufficient to induce apoptosis. Thus, it can be said that, in host H1 and associated clones, the conversion of toxic MGO more rapidly to pyruvate, through an upregulated D-LDHm, could have led to decreased cell death and to a competitive advantage for the host H1 and its resulting clones, compared to H2 and clones.

In summary, selecting for specific phenotypical characteristics in host cells, such as lower aggregation, and/or by manipulating relevant pathway genes, such as Podoplanin, D-LDHm, and others, could potentially result in a richer pool of host cells, from which a "high producer" could be obtained. By using proteomics to investigate and identify characteristics of desirable CHO host cells, this study provides insights into ways to engineer CHO cells to obtain clones with higher protein productivity. This will enable biopharmaceutical companies to improve bioprocessing capabilities of CHO cells while also reducing the time to development of "ideal" CHO hosts and clones.

AUTHOR CONTRIBUTIONS

Swetha Kumar, Amit Kumar, Steven Huhn, Robert Cole, Zhimei Du, and Michael Betenbaugh conceived and designed the research. Swetha Kumar, Amit Kumar, Steven Huhn, and Lauren DeVine conducted experiments. Swetha Kumar, Amit Kumar, and Michael Betenbaugh analyzed data. Swetha Kumar, Amit Kumar, Steven Huhn, Lauren DeVine, and Michael Betenbaugh wrote the manuscript. All authors have given approval to the final version of the manuscript.

ACKNOWLEDGMENT

CONFLICTS OF INTEREST

The authors declare no conflicts of interest.

DATA AVAILABILITY STATEMENT

The analyzed data that support the findings of this study are available in the supplementary materials of this article.

ORCID

Swetha Kumar http://orcid.org/0000-0002-3740-7977
Amit Kumar http://orcid.org/0000-0003-2140-5130
Steven Huhn http://orcid.org/0000-0002-7826-5610
Lauren DeVine http://orcid.org/0000-0002-9838-0704
Robert Cole http://orcid.org/0000-0002-3096-4754
Michael Betenbaugh http://orcid.org/0000-0002-6336-4659

REFERENCES

Astarita, J. L., Acton, S. E., & Turley, S. J. (2012). Podoplanin: Emerging functions in development, the immune system, and cancer. *Frontiers in Immunology*, 3, 1–11. https://doi.org/10.3389/fimmu.2012.00283

Baycin-Hizal, D., Tabb, D. L., Chaerkady, R., Chen, L., Lewis, N. E., Nagarajan, H., Sarkaria, V., Kumar, A., Wolozny, D., Colao, C., Jacobson, E., Tian, Y., O'Meally, R. N., Krag, S. S., Cole, R. N., Palsson, B. O., Zhang, H., & Betenbaugh, M. (2013). Proteomic analysis of Chinese hamster ovary cells. *Journal of Proteome Research*, 11(11), 5265–5276. https://doi.org/10.1021/pr300476w

Blondeel, E. J. M., Ho, R., Schulze, S., Sokolenko, S., Guillemette, S. R., Slivac, I., Durocher, Y., Guillemette, J. G., McConkey, B. J., Chang, D., & Aucoin, M. G. (2016). An omics approach to rational feed: Enhancing growth in CHO cultures with NMR metabolomics and 2D-DIGE proteomics. *Journal of Biotechnology*, 234, 127–138. https://doi.org/10.1016/j.jbiotec.2016.07.027

Chandra, D., Liu, J. W., & Tang, D. G. (2002). Early mitochondrial activation and cytochrome c up-regulation during apoptosis. *Journal of Biological Chemistry*, 277(52), 50842–50854. https://doi.org/10.1074/jbc.M207622200

Chang, M., Kumar, A., Kumar, S., Huhn, S., Timp, W., Betenbaugh, M., & Du, Z. (2022). Epigenetic comparison of CHO hosts and clones reveals divergent methylation and transcription patterns across lineages. *Biotechnology and Bioengineering*, 119, 1062–1076. https://doi.org/10.1002/bit.28036

Chaplen, F. W. R., Fahl, W. E., & Cameron, D. C. (1996). Effect of endogenous methylglyoxal on Chinese hamster ovary cells grown in culture. *Cytotechnology*, 22(1–3), 33–42. https://doi.org/10.1007/BF00353922

Chiquet-Ehrismann, R. (1995). Inhibition of cell adhesion by anti-adhesive molecules. *Current Opinion in Cell Biology*, 7(5), 715–719. https://doi.org/10.1016/0955-0674(95)80114-6

Cho, Z., Konishi, E., Kanemaru, M., Isohisa, T., Arita, T., Kawai, M., Tsutsumi, M., Mizutani, H., Takenaka, H., Ozawa, T., Tsuruta, D., Katoh, N., & Asai, J. (2017). Podoplanin expression in peritumoral keratinocytes predicts aggressive behavior in extramammary Paget's disease. *Journal of Dermatological Science*, 87(1), 29–35. https://doi.org/10.1016/j.jdermsci.2017.03.012

Cueni, L. N., & Detmar, M. (2009). Galectin-8 interacts with podoplanin and modulates lymphatic endothelial cell functions. *Experimental Cell Research*, 315(10), 1715–1723. https://doi.org/10.1016/j.yexcr.2009.02.021

Dahodwala, H., & Sharfstein, S. T. (2017). The 'omics revolution in CHO biology: Roadmap to improved CHO productivity. In: P. Meleady (Ed.), Heterologous protein production in CHO cells: Methods and protocols. *Methods in molecular biology* (Vol. 1603, pp. 153–168). Humana Press. http://www.springer.com/series/7651

De Bari, L., Atlante, A., Guaragnella, N., Principato, G., & Passarella, S. (2002). D-lactate transport and metabolism in rat liver mitochondria. *Biochemical Journal*, 365(2), 391–403. https://doi.org/10.1042/BJ20020139

Dhara, V. G., Naik, H. M., Majewska, N. I., & Betenbaugh, M. J. (2018). Recombinant antibody production in CHO and NS0 cells:

Differences and similarities. *BioDrugs*, *32*(6), 571–584. https://doi.org/10.1007/s40259-018-0319-9

Doolan, P., Clarke, C., Kinsella, P., Breen, L., Meleady, P., Leonard, M., Zhang, L., Clynes, M., Aherne, S. T., & Barron, N. (2013). Transcriptomic analysis of clonal growth rate variation during CHO cell line development. *Journal of Biotechnology*, *166*(3), 105–113. https://doi.org/10.1016/j.jbiotec.2013.04.014

Ewaschuk, J. B., Naylor, J. M., & Zello, G. A. (2005). D-lactate in human and ruminant metabolism. *Journal of Nutrition*, *135*(7), 1619–1625. https://doi.org/10.1093/jn/135.7.1619

Farrell, A., McLoughlin, N., Milne, J. J., Marison, I. W., & Bones, J. (2014). Application of multi-omics techniques for bioprocess design and optimization in Chinese hamster ovary cells. *Journal of Proteome Research*, *13*(7), 3144–3159. https://doi.org/10.1021/pr500219b

Flick, M. J., & Konieczny, S. F. (2002). Identification of putative mammalian. *Biochemical and Biophysical Research Communications*, *295*, 910–916.

Geiger, B., Bershadsky, A., Pankov, R., & Yamada, K. M. (2001). Transmembrane extracellular matrix-cytoskeleton crosstalk. *Nature Reviews Molecular Cell Biology*, *2*(11), 793–805. https://doi.org/10.1038/35099066

Guay, C., Joly, É., Pepin, É., Barbeau, A., Hentsch, L., Pineda, M., Madiraju, S. R. M., Brunengraber, H., & Prentki, M. (2013). A role for cytosolic isocitrate dehydrogenase as a negative regulator of glucose signaling for insulin secretion in pancreatic ß-cells. *PLoS One*, *8*(10), e77097. https://doi.org/10.1371/journal.pone.0077097

Heffner, K., Hizal, D. B., Majewska, N. I., Kumar, S., Dhara, V. G., Zhu, J., Bowen, M., Hatton, D., Yerganian, G., Yerganian, A., O'Meally, R., Cole, R., & Betenbaugh, M. (2020). Expanded Chinese hamster organ and cell line proteomics profiling reveals tissue-specific functionalities. *Scientific Reports*, *10*(1), 1–12. https://doi.org/10.1038/s41598-020-72959-8

Huhn, S. C., Ou, Y., Kumar, A., Liu, R., & Du, Z. (2019). High throughput, efficacious gene editing & genome surveillance in Chinese hamster ovary cells. *PLoS One*, *14*(12), 1–14. https://doi.org/10.1371/journal.pone.0218653

Jenkins, N., Castro, P., Menon, S., Ison, A., & Bull, A. (1994). Effect of lipid supplements on the production and glycosylation of recombinant interferon-γ expressed in CHO cells. *Cytotechnology*, *15*(1–3), 209–215. https://doi.org/10.1007/BF00762395

Kazemi Seresht, A., Cruz, A. L., De Hulster, E., Hebly, M., Palmqvist, E. A., Van Gulik, W., Daran, J. M., Pronk, J., & Olsson, L. (2013). Long-term adaptation of *Saccharomyces cerevisiae* to the burden of recombinant insulin production. *Biotechnology and Bioengineering*, *110*(10), 2749–2763. https://doi.org/10.1002/bit.24927

Kelley, B. (2020). Developing therapeutic monoclonal antibodies at pandemic pace. *Nature Biotechnology*, *38*(5), 540–545. https://doi.org/10.1038/s41587-020-0512-5

Kildegaard, H. F., Baycin-Hizal, D., Lewis, N. E., & Betenbaugh, M. J. (2013). The emerging CHO systems biology era: Harnessing the'omics revolution for biotechnology. *Current Opinion in Biotechnology*, *24*(6), 1102–1107. https://doi.org/10.1016/j.copbio.2013.02.007

Kingkeohoi, S., & Chaplen, F. W. R. (2005). Analysis of methylglyoxal metabolism in CHO cells grown in culture. *Cytotechnology*, *48*(1–3), 1–13. https://doi.org/10.1007/s10616-005-1920-6

Koh, H. J., Lee, S. M., Son, B. G., Lee, S. H., Ryoo, Z. Y., Chang, K. T., Park, J. W., Park, D. C., Song, B. J., Veech, R. L., Song, H., & Huh, T. L. (2004). Cytosolic NADP+-dependent isocitrate dehydrogenase plays a key role in lipid metabolism. *Journal of Biological Chemistry*, *279*(38), 39968–39974. https://doi.org/10.1074/jbc.M402260200

Kumar, S., Dhara, V. G., Orzolek, L. D., Hao, H., More, A. J., Lau, E. C., & Betenbaugh, M. J. (2020). Elucidating the impact of cottonseed hydrolysates on CHO cell culture performance through

transcriptomic analysis. *Applied Microbiology and Biotechnology*, *105*, 271–285. https://doi.org/10.1007/s00253-020-10972-7

Kunita, A., Kashima, T. G., Morishita, Y., Fukayama, M., Kato, Y., Tsuruo, T., & Fujita, N. (2007). The platelet aggregation-inducing factor aggrus/podoplanin promotes pulmonary metastasis. *American Journal of Pathology*, *170*(4), 1337–1347. https://doi.org/10.2353/ajpath.2007.060790

Ley, D., Seresht, A. K., Engmark, M., Magdenoska, O., Nielsen, K. F., Kildegaard, H. F., & Andersen, M. R. (2015). Multi-omic profiling -of EPO-producing Chinese hamster ovary cell panel reveals metabolic adaptation to heterologous protein production. *Biotechnology and Bioengineering*, *112*(11), 2373–2387. https://doi.org/10.1002/bit.25652

Müller, B., Heinrich, C., Jabs, W., Kaspar-Schönefeld, S., Schmidt, A., Rodrigues de Carvalho, N., Albaum, S. P., Baessmann, C., Noll, T., & Hoffrogge, R. (2017). Label-free protein quantification of sodium butyrate treated CHO cells by ESI-UHR-TOF-MS. *Journal of Biotechnology*, *257*, 87–98. https://doi.org/10.1016/j.jbiotec.2017.03.032

Parsons, J. T., Horwitz, A. R., & Schwartz, M. A. (2010). Cell adhesion: Integrating cytoskeletal dynamics and cellular tension. *Nature Reviews Molecular Cell Biology*, *11*(9), 633–643. https://doi.org/10.1038/nrm2957

Renner, W. A., Jordan, M., Eppenberger, H. M., & Leist, C. (1993). Cell–cell adhesion and aggregation: Influence on the growth behavior of CHO cells. *Biotechnology and Bioengineering*, *41*(2), 188–193. https://doi.org/10.1002/bit.260410204

Richelle, A., & Lewis, N. E. (2017). Improvements in protein production in mammalian cells from targeted metabolic engineering. *Current Opinion in Systems Biology*, *6*, 1–6. https://doi.org/10.1016/j.coisb.2017.05.019

Schelletter, L., Albaum, S., Walter, S., Noll, T., & Hoffrogge, R. (2019). Clonal variations in CHO IGF signaling investigated by SILAC-based phosphoproteomics and LFQ-MS. *Applied Microbiology and Biotechnology*, *103*(19), 8127–8143. https://doi.org/10.1007/s00253-019-10020-z

Singh, A., Kildegaard, H. F., & Andersen, M. R. (2018). An online compendium of CHO RNA-seq data allows identification of CHO cell line-specific transcriptomic signatures. *Biotechnology Journal*, *13*(10), 1–11. https://doi.org/10.1002/biot.201800070

Sommeregger, W., Mayrhofer, P., Steinfellner, W., Reinhart, D., Henry, M., Clynes, M., Meleady, P., & Kunert, R. (2016). Proteomic differences in recombinant CHO cells producing two similar antibody fragments. *Biotechnology and Bioengineering*, *113*(9), 1902–1912. https://doi.org/10.1002/bit.25957

Stolfa, G., Smonskey, M. T., Boniface, R., Hachmann, A. B., Gulde, P., Joshi, A. D., Pierce, A. P., Jacobia, S. J., & Campbell, A. (2018). CHO-omics review: The impact of current and emerging technologies on Chinese hamster ovary based bioproduction. *Biotechnology Journal*, *13*(3), 1–14. https://doi.org/10.1002/biot.201700227

Suzuki-Inoue, K., Kato, Y., Inoue, O., Mika, K. K., Mishima, K., Yatomi, Y., Yamazaki, Y., Narimatsu, H., & Ozaki, Y. (2007). Involvement of the snake toxin receptor CLEC-2, in podoplanin-mediated platelet activation, by cancer cells. *Journal of Biological Chemistry*, *282*(36), 25993–26001. https://doi.org/10.1074/jbc.M702327200

Talasniemi, J. P., Pennanen, S., Savolainen, H., Niskanen, L., & Liesivuori, J. (2008). Analytical investigation: Assay of d-lactate in diabetic plasma and urine. *Clinical Biochemistry*, *41*(13), 1099–1103. https://doi.org/10.1016/j.clinbiochem.2008.06.011

Tejchman, A., Lamerant-Fayel, N., Jacquinet, J. C., Bielawska-Pohl, A., Mleczko-Sanecka, K., Grillon, C., Chouaib, S., Ugorski, M., & Kieda, C. (2017). Tumor hypoxia modulates podoplanin/CCL21 interactions in CCR7+ NK cell recruitment and CCR7+ tumor cell mobilization. *Oncotarget*, *8*(19), 31876–31887. https://doi.org/10.18632/oncotarget.16311

Tönjes, M., Barbus, S., Park, Y. J., Wang, W., Schlotter, M., Lindroth, A. M., Pleier, S. V., Bai, A. H. C., Karra, D., Piro, R. M., Felsberg, J., Addington, A., Lemke, D., Weibrecht, I., Hovestadt, V., Rolli, C. G., Campos, B., Turcan, S., Sturm, D., & Radlwimmer, B. (2013). BCAT1

promotes cell proliferation through amino acid catabolism in gliomas carrying wild-type IDH1. *Nature Medicine*, *19*(7), 901–908. https://doi.org/10.1038/nm.3217

Ugorski, M., Dziegiel, P., & Suchanski, J. (2016). Podoplanin—A small glycoprotein with many faces. *American Journal of Cancer Research*, *6*(2), 370–386.

Uribarri, J., Oh, M. S., & Carroll, H. J. (1998). D-lactic acidosis: A review of clinical presentation, biochemical features, and pathophysiologic mechanisms. *Medicine*, *77*(2), 73–82. https://doi.org/10.1097/00005792-199803000-00001

Welchen, E., Schmitz, J., Fuchs, P., García, L., Wagner, S., Wienstroer, J., Schertl, P., Braun, H. P., Schwarzländer, M., Gonzalez, D. H., & Maurino, V. G. (2016). D-lactate dehydrogenase links methylglyoxal degradation and electron transport through cytochrome. *Plant Physiology*, *172*(2), 901–912. https://doi.org/10.1104/pp.16.01174

Zhou, Y., Zhou, B., Pache, L., Chang, M., Khodabakhshi, A. H., Tanaseichuk, O., Benner, C., & Chanda, S. K. (2019). Metascape provides a biologist-oriented resource for the analysis of systems-level datasets. *Nature Communications*, *10*(1), 1523. https://doi.org/10.1038/s41467-019-09234-6

SUPPORTING INFORMATION

Additional supporting information can be found online in the Supporting Information section at the end of this article.